J Mater Sci (2010) 45:3175–3183
DOI 10.1007/s10853-010-4324-8

Microwave sintering improves the mechanical properties of biphasic calcium phosphates from hydroxyapatite microspheres produced from hydrothermal processing

Dj. Veljović · E. Palcevskis · A. Dindune · S. Putić · I. Balać · R. Petrović · Dj. Janaćković

Received: 21 September 2009 / Accepted: 13 February 2010 / Published online: 2 March 2010

Abstract Starting from two microspherical agglomerated HAP powders, porous biphasic HAP/TCP bioceramics were obtained by microwave sintering. During the sintering the HAP powders turned into biphasic mixtures, whereby HAP was the dominant crystalline phase in the case of the sample with the higher Ca/P ratio (HAP1) while α-TCP was the dominant crystalline phase in the sample with lower Ca/P ratio (HAP2). The porous microstructures of the obtained bioceramics were characterized by spherical intra-agglomerate pores and shapeless inter-agglomerate pores. The fracture toughness of the HAP1 and HAP2 samples microwave sintered at 1200 °C for 15 min were 1.25 MPa $m^{1/2}$. The phase composition of the obtained bioceramics only had a minor effect on the indentation fracture toughness compared to a unique microstructure consisting of spherical intra-agglomerate pores with strong bonds between the spherical agglomerates. Cold isostatic pressing at 400 MPa before microwave sintering led to an increase in the fracture toughness of the biphasic HAP/TCP bioceramics to 1.35 MPa $m^{1/2}$.

Dj. Veljović (✉) · S. Putić · R. Petrović · Dj. Janaćković
Faculty of Technology and Metallurgy, University of Belgrade, Karnegijeva 4, 11120 Belgrade, Serbia
e-mail: djveljovic@tmf.bg.ac.rs

E. Palcevskis · A. Dindune
Institute of Inorganic Chemistry, Riga Technical University, Miera 34, Salaspils, LV-2169 Riga, Latvia

I. Balać
Faculty of Mechanical Engineering, University of Belgrade, Kraljice Marije 16, 11120 Belgrade, Serbia

Introduction

Bioceramics based on hydroxyapatite (HAP, $Ca_{10}(PO_4)_6(OH)_2$) and tricalcium phosphate (α- and β-TCP, $Ca_3(PO_4)_2$), have great potential for biomedical applications because of their chemical composition, osteoconduction, excellent bioactivity, and biocompatibility [1]. As their compositions are similar to the mineral part of bone, calcium phosphate ceramic materials are used today as particular prosthetic components, dental and maxillofacial implants and restorations, bone fillers and scaffolds for tissue engineering [2, 3].

Dense, porous, and scaffold sintered forms of such phosphate ceramics are generally used in clinical practice but most of the current bone substitutes are porous pieces of HAP/TCP composites [4, 5]. Porous HAP materials improve the mechanical interlock between the cells and the surface of the material and promote osteoconductivity [6]. Porous ceramics have attracted a great deal of attention for applications in tissue engineering and drug delivery systems [7, 8]. Careful control of the macro and micro porosities of sintered bioceramic materials in accordance with good mechanical properties can be a key issue for a successful implant. The macro porosity controls access of tissues and biological fluids to the volume of the substitute, while the micro porosity influences adhesion of cells and the resorption rate of calcium phosphate.

A large number of studies were focused on determining the conditions required to obtain a HAP/TCP form suitable for incorporation in living bone [9–11]. Even though the bioactivity and biocompatibility of HAP and TCP are excellent, their brittle nature and bad mechanical properties, especially in wet environments as found under physiological conditions, limit the employment of these materials in load-bearing clinical application. Numerous

efforts have been made to develop bioceramic porous microstructures which improve the mechanical properties of HAP-based materials.

Bioceramic materials based on HAP are usually obtained by pressing and conventional sintering of different HAP powders [12–14]. The high sintering temperatures and long sintering duration required for consolidation of HAP powders often result in extreme grain coarsening, which is characteristic for conventional sintering methods, resulting in the deterioration of the mechanical properties of the ceramics [15, 16]. The microwave sintering technique shows great potential in ceramics processing [17, 18]. This technique may lead to a series of benefits, including great microstructure control, no limit in geometry of the product, improved mechanical properties of the final materials, and reduced manufacture costs due to energy savings, lower temperatures of sintering and shorter processing times.

Microwave sintering of calcium hydroxyapatite was first reported by Fang et al [19, 20]. Microwave heating is a fast sintering process fundamentally different from conventional radiant element techniques in that the energy can be deposited volumetrically throughout the material rather than relying on thermal conduction from the surface [21]. Conventional furnaces heat the samples by the surface heating mechanism. During heating, a large thermal gradient from the surface to the center can be generated within a sample, especially in the case of the materials with poor thermal conductivity. However, the volumetric heating through microwave treatment ensures uniform heating and almost no thermal gradient, which allows higher heating rates and reduces the processing time.

Sintering of HAP is a complex process since many parameters influence the sintering process. Different methods of syntheses, such as solid-state reaction, modified chemical precipitation methods, sol–gel synthesis, ultrasonic spray-pyrolysis, catalytic decomposition of urea with urease, hydrothermal decomposition of urea, and calcium-EDTA chelates, etc., have been exploited to synthesize HAP powders in attempts to obtain different sintered forms with good mechanical properties [22–26]. The mechanical properties and microstructures of the resulting HAP ceramics are strictly linked to the characteristics of the original HAP powder, including crystallinity, agglomeration, stoichiometry, substitutions, and on the processing conditions [27, 28]. Nano-sized HAP powders are often agglomerated as a consequence of their high surface energy, whereby the size and shape of the agglomerates are dependent on the synthesis parameters. Synthesis of agglomerate-free and slightly agglomerated HAP powders can be an important step toward obtaining dense materials [14, 15]. However, the synthesis of hard spherical micro-agglomerated spherical powders can be an essential step for the processing of porous-sintered bioceramics with controlled size and shapes of the pores. Changes in the mechanical properties of porous sintered HAP materials are correlated with phase transformation during sintering, grain sizes, bonding between the grains, density, and pore size and shape. The effect of porosity, especially spherical intra-agglomerate pores, on the mechanical properties (mainly fracture toughness) of porous-sintered bioceramics based on HAP constitutes an increase in the path length, thereby creating a highly torturous crack path, with increased energy absorption during crack propagation [8, 29].

The aims of this work were to study the processing and characterization of porous HAP/TCP bioceramics obtained by microwave sintering of two different spherical agglomerated nano-sized HAP powders synthesized by hydrothermal decomposition of urea and calcium-EDTA chelates. The effects of microstructural parameters, processing conditions of the microwave sintering and phase composition on the mechanical properties of controlled porous biomaterials based on HAP and TCP were investigated. The joint effect of high cold isostatic pressing and microwave sintering on the microstructure and mechanical properties of the obtained porous HAP bioceramics was also investigated.

Experimental

Two different calcium hydroxyapatite powders were obtained by modified hydrothermal syntheses [26, 30, 31]. $CaCl_2{\cdot}2H_2O$, $Na_2H_2EDTA{\cdot}2H_2O$, $NaH_2PO_4{\cdot}2H_2O$, and urea were dissolved in 2000 mL of distilled water (Table 1). Two different quantities of $CaCl_2{\cdot}2H_2O$ were used due to vary the Ca/P ratio in the starting solution (Ca/P (HAP1) = 1.42 and Ca/P (HAP2) = 0.96). The solutions were heated in an autoclave at 160 °C for 3 h. After heat treatment, the suspension was filtrated using Buchner funnel, washed with warm distilled water, and then dried at 105 °C for 2 h.

The HAP1 and HAP2 powders were uniaxially pressed at 100 MPa using a stainless steel die into green disc

Table 1 The quantities of the reactants employed for the hydrothermal syntheses of HAP1 and HAP2

	$C_aCl_2{\cdot}2H_2O$(g)	$Na_2H_2EDTA{\cdot}2H_2O$(g)	$Na_2H_2PO_4{\cdot}2H_2O$(g)	$CO(NH_2)_2$ (g)
HAP 1	15.96	14.80	12.00	12.00
HAP2	11.00	14.80	12.00	12.00

compacts, 12 mm in diameter. The first group of green compacts were then sintered in an automated microwave laboratory furnace (Linn High Therm MHTD 1800-4,8/2,45-135) at 900, 1000, 1100, and 1200 °C for 15 min. The heating rate to the desired temperature was 20 °C/min. The temperature of the samples was measured continuously with an optical pyrometer from the top of the furnace. During all the microwave sintering processes, the treated disc samples were at the same place in the microwave furnace, in order to avoid the influence of the geometric factor.

The second group of green compacts were cold isostatically pressed (CIP) at 400 MPa for 1 min. The isostatically green compacts were heated at 20 °C/min and then microwave sintered at 1100 and 1200 °C for 15 min. For comparison isostatically pressed green compacts were conventionally sintered at 1100 and 1200 °C for 2 h, after heating at the same heating rate.

The morphology of the microwave (MW) sintered samples was observed by scanning electron microscopy (SEM) using a Jeol JSM 5800 microscope, operated at 20 keV. The dimensions of the pores were determined by image analysis of the SEM micrographs, using the Image Pro Plus Program, version 4.0 for Windows, software for image analysis. The density of the green samples and sintered samples was determined with the Archimedes method. X-ray diffraction patterns of the HAP powders and sintered compacts were recorded using a Bruker D8 Advance diffractometer with CuK_{α} radiation in the 2θ angle range from 20 to 50° with a step scan of 0.02°.

The microwave sintered compacts were tested for hardness and indentation fracture toughness. The hardness of polished compacts was measured with a Buehler Indentament 1100 series, Vickers Indentation Hardness Tester. The K_{ic} values were calculated using the following formula which was derived from the model proposed by Evans [32]: $K_{ic} = 0.0824\ P{\cdot}c^{-3/2}$, where P is the indentation load and c the length of the induced radial crack.

Results and discussion

Spherical particles of hydroxyapatite powders HAP1 and HAP2 were obtained by hydrothermal syntheses. The SEM micrograph of the HAP1 powder is shown in Fig. 1. The spherical agglomerates of HAP are of uniform size distribution in the size range 2–5 μm. From Fig. 1, it can see that the spherical agglomerates are hollow and that these spherical particles are agglomerates of much smaller rod-shaped nanostructured particles of less than 100 nm in length.

The formation of larger spherical particles from initially formed nanocrystals can be explained by their aggregation.

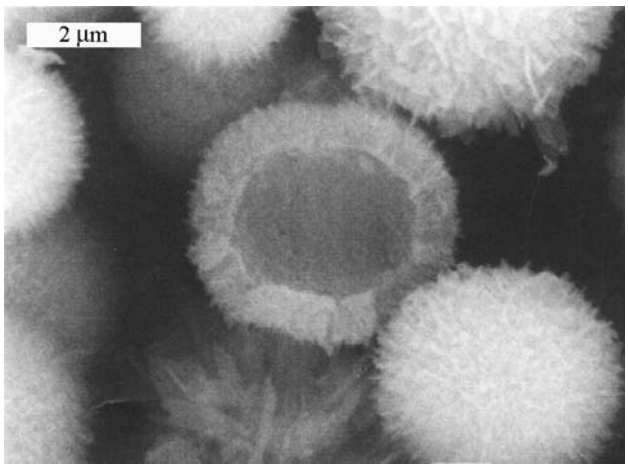

Fig. 1 SEM micrograph of an HAP1 powder

Matijevic et al. [33–38] explained that the formation of uniform particles in colloidal systems often passes through an initial stage or an induction period when the solution reaches saturation point, which leads to particle nucleation. These nuclei further grow by the diffusion mechanism, when the primary particles are formed, followed aggregation to form secondary particles. This second process can be accelerated by changing the synthesis parameters, for instance: by changing the ionic strength or the pH of the solution, which causes a change in the surface charge of the particles, which can come close to or cross the isoelectric point. This effects lead to a lowering of the electrostatic barrier, thereby enabling the aggregation of the primary particles into larger secondary particles.

In the synthesis of the present sample, such synthesis parameters occur. When the initial pH is 3.3, the pH of the solution changes constantly and increases as a consequence of the hydrolysis of urea and attains an end value of about 8.6–8.9. In such a case, the surface charge of the formed primary apatite particles changes, crossing the isoelectric point, and due to a decrease in the surface charge of the particles, they aggregate into larger ones, as a consecvence of the decrease in the surface energy.

The XRD patterns of the HAP1 and HAP2 powders exhibited peaks only corresponding to calcium hydroxyapatite phase (Fig. 2.). All the peaks perfectly matched the JCPDS pattern 9-432 for HAP. The density of the uniaxially pressed green compacts was about 1.40 g/cm^3, i.e., 45% of the theoretical density.

The SEM micrographs of the fracture section of the HAP1 samples MW sintered at 900, 1000, 1100, and 1200 °C are shown in Fig. 3a–d, respectively. Figure 3a shows that the spherical structure of the HAP1 agglomerates was not destroyed after pressing at 100 MPa and MW sintering at 900 °C. There was no bonding between the spherical agglomerates after MW sintering at 900 °C. It

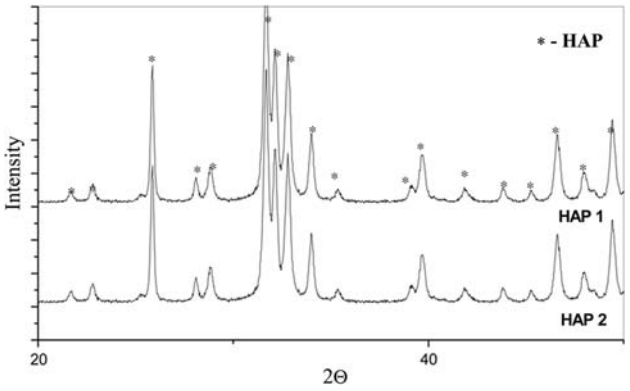

Fig. 2 XRD patterns of the HAP1 and HAP2 powders

can be seen that the subparticles on the surface of the agglomerates were slightly deformed. The SEM micrograph of the HAP1 sample sintered at 1000 °C, Fig. 3b, shows that the spherical agglomerates started to coalesce and bond. It can be seen that the rod-shaped particles at the surface of the agglomerates were rounded and nano-sized spherical grains had formed. At the fracture surface of the compact sintered at 1100 °C, it can definitely be seen that "necks" between the spherical agglomerates had formed (Fig. 3c.). The microstructure was characterized by spherical intra-agglomerate pores and shapeless inter-agglomerate pores. The fracture surface of the samples MW sintered at 1200 °C was characterized by the presence of a slightly higher percent of spherical pores (the amount of inter-agglomerate shapeless pores was lower) and the size of the pores was slightly smaller than those of the compact sintered at 1100 °C (Fig. 3d). Slightly stronger bonds between the agglomerates were formed at 1200 °C.

From the SEM micrographs shown in Fig. 3c, d, it can be seen that the maximum dimension of the pores was defined by the spherical intra-agglomerate pores and that the maximum diameter of the pores of the porous structures is around 2 μm. It can be concluded that the microwave sintering of spherical hard agglomerated HAP powders results in porous bioceramic materials and that the maximum value of the pores depends on the size of the intra-agglomerate pores of the spherical agglomerates.

SEM micrographs of the fracture section of the HAP2 samples MW sintered at 900, 1000, 1100, and 1200 °C are shown in Fig. 3e–h. From Fig. 3e, f it can be seen that the spherical agglomerates of the HAP2 powder started to coalescence at 1000 °C during MW sintering, which was also the case with the HAP1 powder, and also nano-sized grains were formed at the surface of the agglomerates. At the fracture surface of the HAP2 compact sintered at 1100 °C, it can be seen that a porous structure was formed (Fig. 3g), but a more uniform microstructure with a smaller amount of shapeless inter-agglomerate pores was evident at the fracture surface of the compact sintered at 1200 °C (Fig. 3h).

The X-ray patterns of the HAP1 samples microwave sintered at 900, 1000, 1100, and 1200 °C, (Fig. 4a), show peaks suggesting that HAP was the prevailing crystalline phase. A small part of the HAP was transformed into β-TCP at 900 and 1000 °C, while the samples MW sintered at 1100 °C consisted of HAP as the dominant crystalline phase with small amounts of α- and β-TCP. The HAP1 sample MW sintered at 1200 °C consisted of HAP as the prevailing crystalline phase with some α- TCP phase.

The X-ray patterns of the HAP2 samples sintered at 900, 1000, 1100, and 1200 °C (Fig. 4b) show that MW sintering of HAP2 resulted in biphasic HAP/TCP bioceramics. The HAP2 samples obtained at 900 and 1000 °C were also biphasic mixtures of HAP and β-TCP, but a greater part of the HAP had been transformed into β-TCP than was the case with the HAP1 compacts. The XRD pattern of the HAP2 samples MW sintered at 1100 °C showed that an appreciable amount of hydroxyapatite had been converted to α-TCP and that β-TCP was present in only a very low percent. The samples sintered at 1200 °C consisted of α-TCP as the dominant crystalline phase, with small amounts of non-transformed HAP and β-TCP.

The influence of the temperature of MW sintering on the density of the HAP1 and HAP2 compacts is shown in Fig. 5. With increasing temperature from 900 to 1200 °C, the density of the HAP1 samples increased from 1.43 to 2.20 g/cm^3. The densities of the HAP2 compacts sintered at 900–1200 °C were appreciably lower, having values in the range of 1.45–1.96 g/cm^3. Microwave sintering at 1000–1100 °C induced a strong densification of the HAP1 and HAP2 samples. On increasing the temperature to 1200 °C, the density was only slightly increased. The lower densities of the HAP2 samples were due to more intensive phase transformation of HAP (3.15 g/cm^3) to β-TCP (3.07 g/cm^3) and α-TCP (2.84 g/cm^3).

The linear shrinkages of the HAP1 and HAP2 samples are shown in Fig. 6. With increasing temperature from 900 to 1100 °C, the linear shrinkage of the HAP1 samples increased to 17.4 % and in the case of the HAP2 ones to 13.7%. With a further increase in the temperature to 1200 °C, the linear shrinkage of the sample was only slightly higher. The more intensive phase transformation from HAP to TCP in the case of the HAP2 samples could be the main reason for the smaller linear shrinkage of the hydroxyapatite with the lower Ca/P ratio and for the expansion which accompanies the phase transformation from HAP into a TCP phase. These results confirmed the slightly lower densification of the HAP powder with the lower Ca/P ratio.

The hardness of the HAP1 and HAP2 processed porous bioceramics is shown in Fig. 7 as a function of the MW

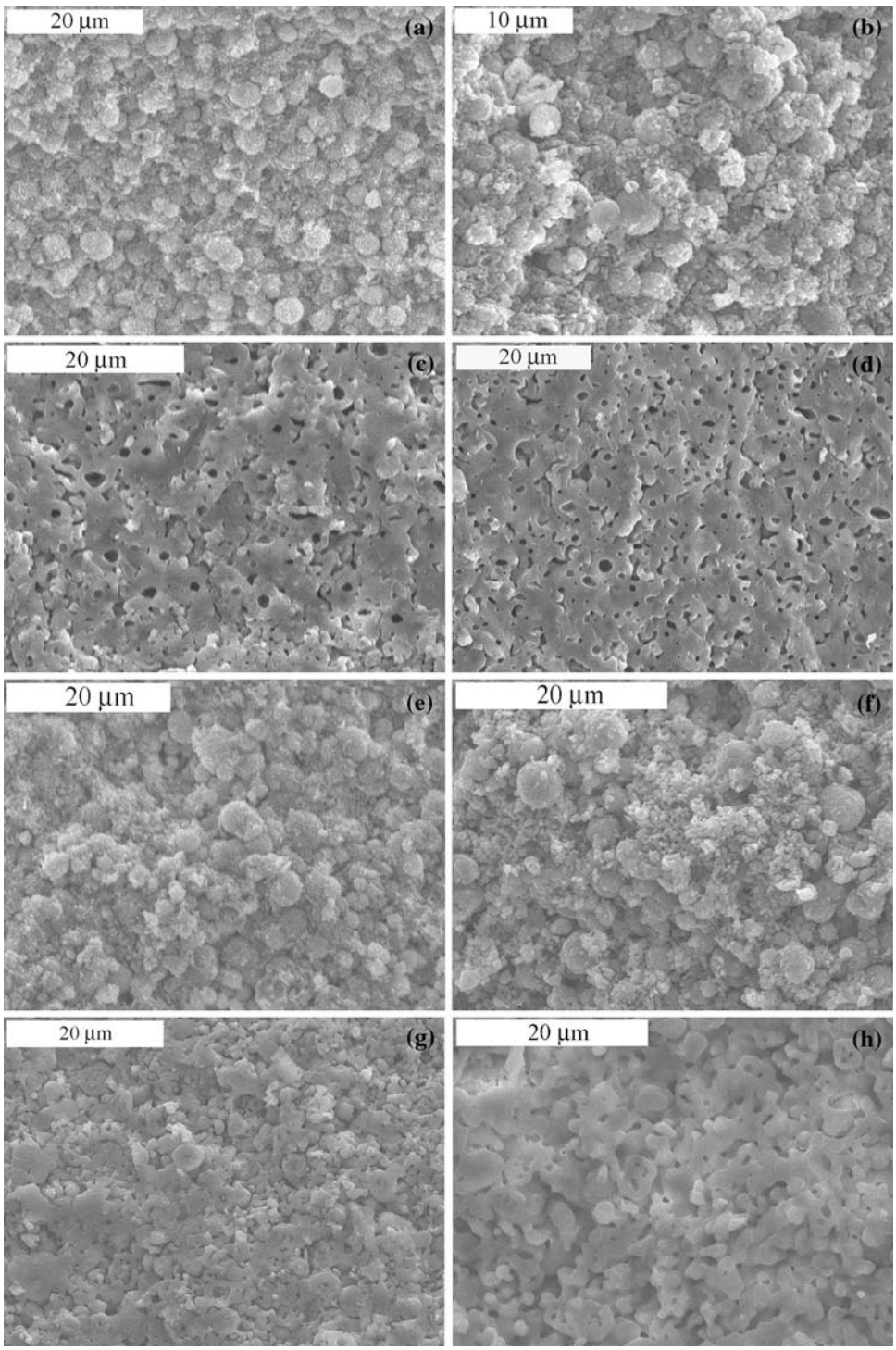

Fig. 3 Micrographs of **a**–**d** HAP1 and **e**–**h** HAP2 MW sintered at different temperatures in the range of 900–1200 °C reveal an increase in density with temperature (**a**, **e**—900 °C, **b**, **f**—1000 °C, **c**, **g**—1100 °C, **d**, **h**—1200 °C)

sintering temperature. Increasing the sintering temperature from 900 to 1200 °C led to an increase of the hardness to 2.70 GPa for HAP1 and to 1.80 GPa in the case of HAP2. The more intensive phase transformation from HAP to TCP and the higher expansion in the case of HAP2 can induce important residual stresses within the densified material, which could be the reason for the lower hardness of the HAP2 bioceramics.

In brittle ceramic materials based on HAP, the fracture toughness is very low, hence after the critical load, processes of surface fracture generation consume more energy while the volume deformation process remains unchanged [39, 40]. Major advances have been made in the development of bioceramic microstructures which increase the energy absorption during crack propagation. Significant improvements to the fracture toughness of ceramic

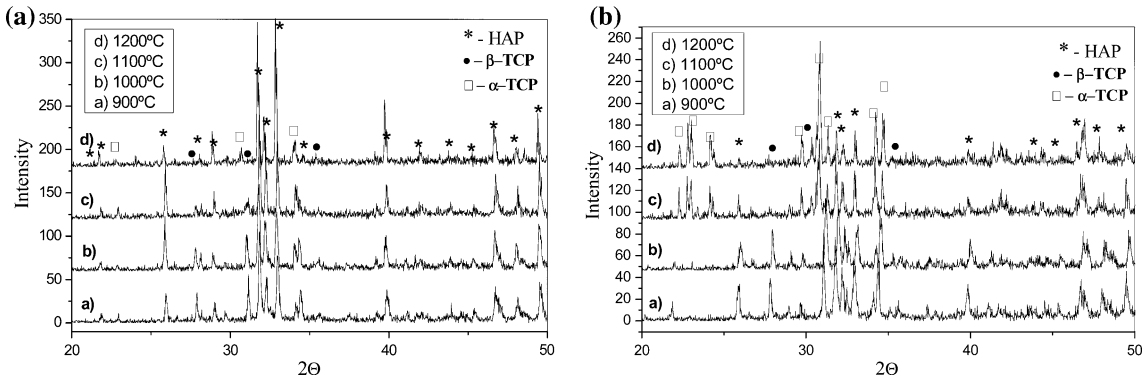

Fig. 4 XRD patterns of **a** HAP1 and **b** HAP2 samples MW sintered at 900–1200 °C

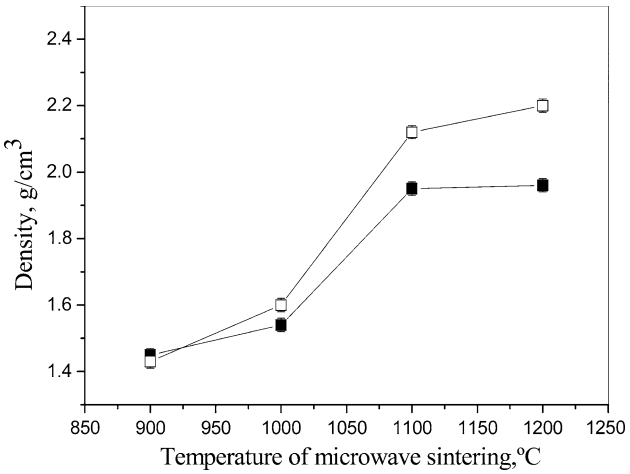

Fig. 5 The density of the HAP1 (□) and HAP2 (■) compacts as a function of the microwave sintering temperature

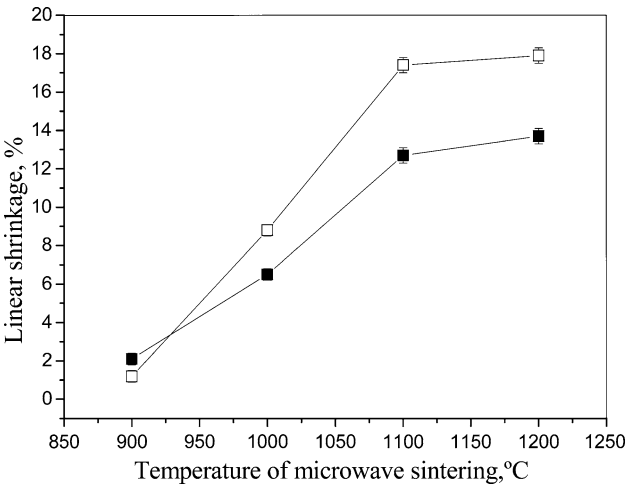

Fig. 6 Linear shrinkage of HAP1 (□) and HAP2 (■) samples microwave sintered at different temperatures

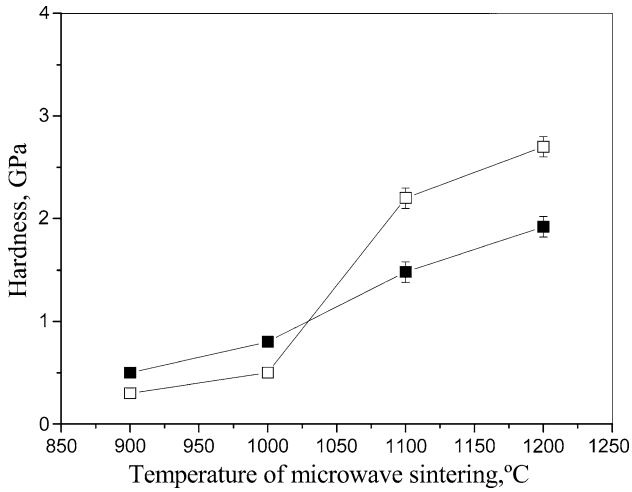

Fig. 7 The hardness of HAP1 (□) and HAP2 (■) samples as a function of microwave sintering temperature

biomaterials through control of the microstructure can be attributed to a combination of several toughening mechanisms, i.e., control of the grain size, control of pores size and shape, etc. [8, 15, 41–44]. Tancret et al. announced that is necessary to optimize the mechanical properties of the porous calcium phosphate bone substitutes and that a compromise must be found between porosities and mechanical properties. By combining two approaches on two different scales, one for closed porosity and one for open porosity, a model was established to describe mechanical properties, among the rest the fracture toughness, as a function of the amount and morphology of the porosity [45]. From all aspects and the established model, it is clear that the amount, size, and morphology of the porosity must be precisely balanced and controlled in order to optimize the overall mechanical performance of these types of bioceramics.

The fracture toughness of the obtained porous bioceramics as a function of the sintering temperature is presented in Fig. 8. The fracture toughness of both types of HAP compacts microwave sintered at 900 and 1000 °C was very low, in the range from 0.35 to 0.50 MPa $m^{1/2}$. Increasing the sintering temperature from 1000 to 1200 °C led to an appreciable increase of the fracture toughness to

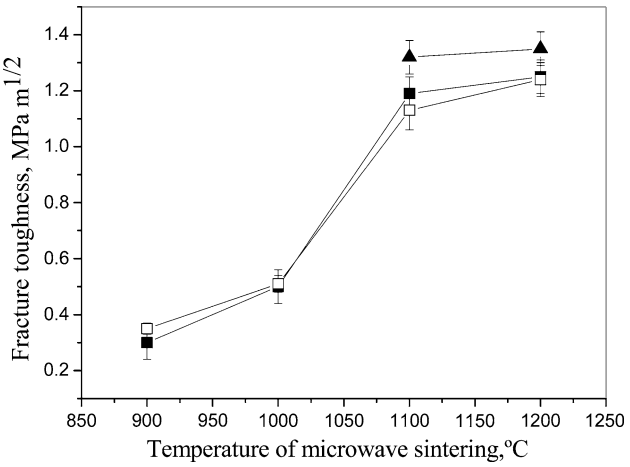

Fig. 8 The fracture toughness of: HAP1 (□), HAP2 (■), and CIP HAP2 (▲) samples as a function of the MW sintering temperature

1.25 MPa $m^{1/2}$ for HAP1 and to 1.25 MPa $m^{1/2}$ for the HAP2 porous compacts (Fig. 8). The indentation fracture toughness of the HAP1 and HAP2 compacts obtained in this study was appreciably higher than those reported in many studies for porous and dense HAP ceramics. Thus, Banerjee et al. [46] found fracture toughnesses ranging from 0.6 to 1.0 MPa $m^{1/2}$ for dense HAP ceramics prepared using conventional sintering, Raynaud et al. [47, 48] measured a fracture toughness of 1.0 MPa $m^{1/2}$ in a hot pressed HAP-based bioceramics and Thangamania et al. [39] obtained an HAP-based bioceramic material with a maximum indentation fracture toughness value of 0.88 MPa $m^{1/2}$. In general, the fracture toughness values for most HAP bioceramics reported in the literature varied between 0.60 and 1 MPa $m^{1/2}$.

The fracture toughnesses of the HAP1 (prevailing crystalline phase was hydroxyapatite) and the HAP2 (prevailing crystalline phase was α-TCP) MW sintered compacts prepared in the present study were the same. The conclusion could be drawn that the phase composition of the porous bioceramics obtained in this study had a minor effect on the indentation fracture toughness compared to a unique microstructure of spherical pores and strong bonding between the spherical agglomerates. The formation of continuous and strong interfaces between the spherical agglomerates MW sintered at 1100 °C increased the fracture toughness because crack propagation is associated with the creation of two new surfaces. As seen from the results (Figs. 3 and 8), the fracture toughness was directly related to the type of porosity. The slightly higher amount of spherical pores at the fracture surface of the compact sintered at 1200 °C compared to the sample sintered at 1100 °C could be the reason for the slightly increased of fracture toughness. The greatest benefit for the fracture toughness of the compacts MW sintered at temperatures higher than 1100 °C could be attributed to their unique microstructure with spherical intra-agglomerate pores. The effect of spherical inter-agglomerate pores on the fracture toughness of the porous sintered bioceramics based on HAP is an increase in path length, which would create a highly torturous crack path and a corresponding increase in the absorption of energy during crack propagation [8]. The controlled morphology and this kind of unique microstructure, due to necessary biological function of porosity, in accordance with good mechanical properties of these bioceramic materials, could be a key issue for a successful implant.

α-TCP, as the dominant phase in the HAP2 samples, has excellent bioactivity, biocompatibility, and due to its resorbability, has an important role in biomedical applications [6]. In order to improve the mechanical properties of the HAP2 samples, the porous ceramic microspherical HAP2 powder was isostatically pressed at 400 MPa and the density of the pressed green compacts was 1.83 g/cm^3, i.e., 58% of the theoretical density. This density was 13 % of the theoretical density higher then the density of the samples uniaxially pressed at 100 MPa. The high green density and intimate contact between the spherical agglomerates can be an important step in the processing of porous bioceramics with improved mechanical properties.

The isostatically pressed HAP2 green compacts were then microwave sintered at 1100 and 1200 °C for 15 min. The microstructures of the fracture surfaces of these samples are shown in Fig. 9a, b, respectively.

These micrographs show that uniform- and fine-grained microstructures were obtained. The density of the CIP sample MW sintered at 1100 °C was 2.60 g/cm^3 and on increasing the temperature to 1200 °C, the density increased to 2.70 g/cm^3 (Table 2). By comparing these results with the SEM micrographs (Fig. 3g, h.) and the density of the HAP2 MW sintered compacts uniaxially pressed at 100 MPa, it can concluded that the MW sintered CIP samples clearly had a higher densification, that stronger bondings between the spherical agglomerates were formed and the pore sizes were smaller.

The fracture toughness of the CIP HAP2 sample MW sintered at 1100 °C was 1.32 MPa $m^{1/2}$ and on increasing the temperature to 1200 °C, the fracture toughness increased to 1.35 MPa $m^{1/2}$ (Fig. 8, Table 2). The hardness of the CIP HAP2 sample MW sintered also increased on increasing the sintering temperature. According to these results, it can be concluded that the combination of cold isostatic pressing of spherical HAP particles and MW sintering could result in HAP/TCP bioceramics with undoubtedly improved mechanical properties, due to the higher densification and stronger bonding between the spherical agglomerates.

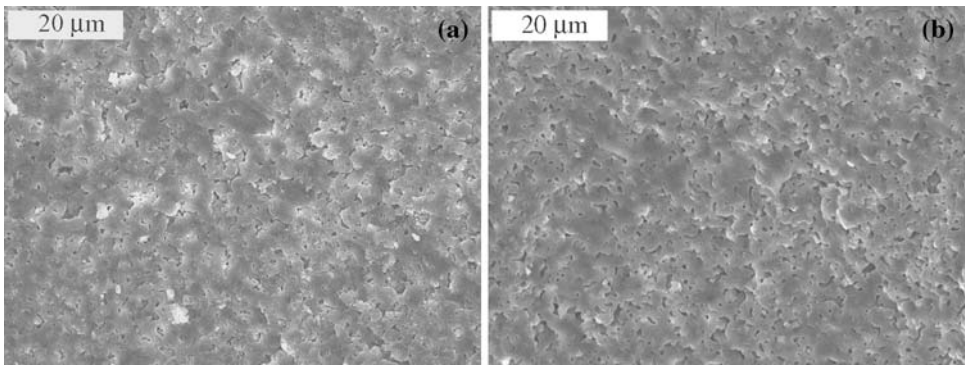

Fig. 9 SEM micrograph of a CIP HAP2 sample MW sintered at **a** 1100 °C and **b** 1200 °C

Table 2 Processing conditions and properties of CIP HAP2 bioceramic materials obtained by conventional and microwave sintering

Temperature of sintering °C	1100	1100	1200	1200
Type of sintering	Conventional	Microwave	Conventional	Microwave
Holding time, min	120	15	120	15
Density, g/cm^3	2.54	2.60	2.62	2.70
Hardness, GPa	2.25	2.45	2.35	2.55
Fracture toughness, MPa/m$^{1/2}$	0.88	1.32	1.20	1.35

In order to observe the effect of the microwaves on the sintering of the CIP HAP2 samples, isostatically pressed green samples were also conventionally sintered at 1100 and at 1200 °C for 2 h. The densities of these samples were slightly lower than the samples CIP and then MW sintered at the same temperatures (Table 2). The fracture toughness of the HAP2 sample conventionally sintered at 1100 °C was more than 30% lower than the value exhibited by the corresponding sample MW sintered at the same temperature. On increasing the sintering temperature to 1200 °C, the fracture toughness of the conventionally sintered HAP2 samples increased to 1.20 MPa m$^{1/2}$. From these results, it was concluded that the cold isostatically pressed and then MW sintered samples had definitely better mechanical properties than the CIP samples conventionally sintered at the same temperature for an eight times longer holding time.

Conclusions

Starting from two different hydrothermally synthesized spherical hydroxyapatite powders, bioceramics based on hydroxyapatite and tricalcium phosphate were obtained by microwave sintering of green compacts uniaxially pressed at 100 MPa. Both hydroxyapatites were converted during microwave sintering into HAP/TCP biphasic mixtures, whereby HAP was the dominant crystalline phase after sintering of the HAP1 and α-TCP was the prevailing crystalline phase in the HAP2 sintered samples. The microstructures of the obtained porous bioceramics were characterized by spherical intraagglomerate pores and shapeless interagglomerate pores. Increasing the sintering temperature from 900 to 1200 °C led to an increase in the density and the fraction of spherical pores in the material and finally improved the mechanical properties of the HAP-based porous bioceramics. The fracture toughness of the HAP1 and HAP2 samples microwave sintered at 1200 °C for 15 min was 1.25 MPa m$^{1/2}$. These relatively high values of the fracture toughness are the result of unique microstructure having spherical intraagglomerate pores and strong bonding between the spherical agglomerates.

Using cold isostatic pressing and then microwave sintering at 1200 °C led to an increase in the fracture toughness of the HAP2 samples to 1.35 MPa m$^{1/2}$. The samples obtained by microwave sintering were characterized with higher fracture toughness and hardness than samples conventionally sintered at the same temperature for an appreciably longer holding time. Controlled porous HAP and α-TCP-based bioceramics materials with different porosities may be produced by this method, by varying the size of the starting spherical agglomerates of the HAP powders.

Acknowledgements The authors wish to acknowledge the financial support from the Ministry of Science and Technological Development of the Republic of Serbia through projects 142070B and EUREKA E! 3033 Bionanocomposit. The Latvian authors also acknowledge the support of the Ministry of Education and Science of the Republic of Latvia under the EUREKA E! 3033 Bionanocomposit project.

References

1. Hench LL (1991) J Am Ceram Soc 74:1487
2. Chevalier J, Gremillard L (2009) J Eur Ceram Soc 29:1245
3. Descamps M, Hornez JC, Leriche A (2009) J Eur Ceram Soc 29:369
4. Le Geros RZ, Lin S, Rohanizadeh R, Mijares D, Le Geros JP (2003) J Mater Sci Mater Med 14:201
5. Shors EC, Holmes RE (1993) In: Hench LL, Wilson J (eds) An introduction to bioceramics. World Scientific, Singapore
6. Vani R, Girija EK, Elayaraja K, Parthiban SP, Kesavamoorthy R, Kalkura SN (2009) J Mater Sci Mater Med. doi: 10.1007/s10856-008-3480-8
7. Kawata M, Uchida H, Itatani K, Okada I, Koda S, Aizawa M (2004) J Mater Sci Mater Med 15:817
8. Kumar R, Prakash KH, Cheang P, Khor KA (2005) Acta Mater 53:2327
9. Barralet JE, Best S, Bonfield W (2000) J Mater Sci Mater Med 11:719
10. Landi E, Tampieri A, Celotti G, Sprio S (2000) J Eur Ceram Soc 20:2377
11. Ribeiro CC, Barrias CC, Barbosa MA (2006) J Mater Sci Mater Med 17:455
12. Mayo MJ (1997) In: Chow GM, Noskova NI (eds) Nanostructured materials, materials science technology, NATO ASI Series. Kluwer Academic Publishers, Russia
13. Groza JR (1999) Nanostruct Mater 12:987
14. Veljovic Dj, Jokic B, Jankovic-Castvan I, Smiciklas I, Petrovic R, Janackovic Dj (2007) Key Eng Mater 330–332:259
15. Veljovic Dj, Jokic B, Petrovic R, Palcevskis E, Dindune A, Mihailescu IN, Janaćkovic Dj (2009) Ceram Int 35:1407
16. Tang CY, Uskokovic PS, Tsui CP, Veljovic Dj, Petrovic R, Janackovic Dj (2009) Ceram Int 35:2171
17. Wang XL, Fan HS, Xiao YM, Zhang XD (2006) Mater Lett 60:455
18. Vijayan S, Varma H (2002) Mater Lett 56:827
19. Fang Y, Agrawal DK, Roy DM, Roy R (1994) J Mater Res 9:180
20. Sutton WH (1989) Am Ceram Soc Bull 68:376
21. Muralithran G, Ramesh S (2000) Ceram Int 26:221
22. Rao RR, Roopa HN, Kanan TS (1997) J Mater Sci Mater Med 8:511
23. Aizava M, Hanazava T, Itatani K, Howell FS, Kishioka A (1999) J Mater Sci 34:2865. doi:10.1023/A:1004635418655
24. Bose S, Saha SK (2003) J Am Ceram Soc 86:1055
25. Jokic B, Tanaskovic D, Jankovic-Castvan I, Drmanic S, Petrovic R, Janackovic Dj (2007) J Mater Res 22:1156
26. Janaćkovic Dj, Petrovic-Prelevic I, Kostic-Gvozdenovic Lj, Petrovic R, Jokanovic V, Uskovic D (2001) Key Eng Mater 203:192
27. Gross KA, Bhadang KA (2004) Biomaterials 25:1395
28. Gross KA, Rodríguez-Lorenzo LM (2004) Biomaterials 25:1385
29. Prokopiev O, Sevostianov I (2006) Mater Sci Eng A 431:218
30. Fujishiro Y, Sato T, Okuwaki A (1995) J Mater Sci 6:172. doi: 10.1007/BF00120295
31. Jokic B, Jankovic-Castvan I, Veljović Dj, Bucevac D, Obradovic-Djuricic K, Petrovic R, Janackovic Dj (2007) J Opt Adv Mater 9:1904
32. Evans AG, Charles EA (1976) J Am Ceram Soc 59:371
33. Matijevic E (1998) J Eur Ceram Soc 18:1357
34. Privman V, Goia D, Park J, Matijevic E (1999) J Colloid Interface Sci 213:36
35. Goia DV, Matijevic E (1999) Colloids Surf A Physicochem Eng Asp 146:139
36. Park J, Privman V, Matijevic E (2001) J Phys Chem B 105:11630
37. Libert S, Gorshov V, Privman V, Gioa D, Matijevic E (2003) Adv Colloid Interface Sci 100–102:169
38. Sondi I, Matijevic E (2003) Chem Mater 15:1322
39. Thangamania N, Chinnakalib K, Gnanama FD (2002) Ceram Int 28:355
40. Lawn BR, Jensen T, Arora A (1976) J Mater Sci Lett 11:573
41. Chiang YM, Birnie DP, Kingery WD (1997) Physical ceramics. Wiley, New York
42. Lawn BR, Marshall DB (1979) J Am Ceram Soc 62:347
43. Landuyt PV, Li F, Keustermans JP, Streydio JM, Delannay F, Munting E (1995) J Mater Sci Mater Med 6:8
44. Callister WD (2003) Materials science and engineering: an introduction. Wiley, New York
45. Tancret F, Bouler JM, Chamousset J, Minois LM (2006) J Eur Ceram Soc 26:3647
46. Banerjee A, Bandyopadhyay A, Bose S (2007) Mater Sci Eng C 27:729
47. Raynaud S, Champion E, Lafon JP, Bernache-Assollant D (2002) Biomaterials 23:1081
48. Raynaud S, Champion E, Bernache-Assollant D (2002) Biomaterials 23:1073